

Original Article

Anatomy/Histology/
Embryology



Chlorogenic acid alleviates the reduction of Akt and Bad phosphorylation and of phospho-Bad and 14-3-3 binding in an animal model of stroke

Murad-Ali Shah ^{1,†}, Ju-Bin Kang ^{1,†}, Myeong-Ok Kim ², Phil-Ok Koh ^{1,*}

¹Department of Anatomy and Histology, College of Veterinary Medicine, Gyeongsang National University, Jinju 52828, Korea

²Division of Life Science and Applied Life Science, College of Natural Sciences, Gyeongsang National University, Jinju 52828, Korea



Received: Jul 27, 2022

Revised: Sep 5, 2022

Accepted: Sep 15, 2022

Published online: Sep 30, 2022

*Corresponding author:

Phil-Ok Koh

Department of Anatomy and Histology,
College of Veterinary Medicine, Gyeongsang
National University, 501 Jinju-daero, Jinju
52828, Korea.

Email: pokoh@gnu.ac.kr

https://orcid.org/0000-0003-0091-8287

[†]Murad-Ali Shah and Ju-Bin Kang were equally contributed.

ABSTRACT

Background: Stroke is caused by disruption of blood supply and results in permanent disabilities as well as death. Chlorogenic acid is a phenolic compound found in various fruits and coffee and exerts antioxidant, anti-inflammatory, and anti-apoptotic effects.

Objectives: The purpose of this study was to investigate whether chlorogenic acid regulates the PI3K-Akt-Bad signaling pathway in middle cerebral artery occlusion (MCAO)-induced damage.

Methods: Chlorogenic acid (30 mg/kg) or vehicle was administered peritoneally to adult male rats 2 h after MCAO surgery, and animals were sacrificed 24 h after MCAO surgery. Neurobehavioral tests were performed, and brain tissues were isolated. The cerebral cortex was collected for Western blot and immunoprecipitation analyses.

Results: MCAO damage caused severe neurobehavioral disorders and chlorogenic acid improved the neurological disorders. Chlorogenic acid alleviated the MCAO-induced histopathological changes and decreased the number of terminal deoxynucleotidyl transferase dUTP nick end labeling-positive cells. Furthermore, MCAO-induced damage reduced the expression of phospho-PDK1, phospho-Akt, and phospho-Bad, which was alleviated with administration of chlorogenic acid. The interaction between phospho-Bad and 14-3-3 levels was reduced in MCAO animals, which was attenuated by chlorogenic acid treatment. In addition, chlorogenic acid alleviated the increase of cytochrome c and caspase-3 expression caused by MCAO damage.

Conclusions: The results of the present study showed that chlorogenic acid activates phospho-Akt and phospho-Bad and promotes the interaction between phospho-Bad and 14-3-3 during MCAO damage. In conclusion, chlorogenic acid exerts neuroprotective effects by activating the Akt-Bad signaling pathway and maintaining the interaction between phospho-Bad and 14-3-3 in ischemic stroke model.

Keywords: Chlorogenic acid; ischemic stroke; neuroprotection

© 2022 The Korean Society of Veterinary Science
This is an Open Access article distributed under the
terms of the Creative Commons Attribution Non-
Commercial License (<https://creativecommons.org/licenses/by-nc/4.0>) which permits unrestricted non-
commercial use, distribution, and reproduction in any
medium, provided the original work is properly cited.

ORCID iDs

Murad-Ali Shah

<https://orcid.org/0000-0002-8388-6497>

Ju-Bin Kang

<https://orcid.org/0000-0003-0508-6264>

Myeong-Ok Kim

<https://orcid.org/0000-0003-4317-1072>

Phil-Ok Koh

<https://orcid.org/0000-0003-0091-8287>**Author Contributions**

Conceptualization: Koh PO; Data curation: Kim

MO; Supervision: Koh PO; Visualization: Shah

MA, Kang JB; Writing - original draft: Shah MA.

Conflict of Interest

The authors declare no conflicts of interest.

Funding

This research was supported by the National Research Foundation of Korea (NRF) grant funded by the Korea government (MEST; NRF-2021R1F1A105878711).

INTRODUCTION

Stroke is a serious neurological disorder and the second leading cause of death [1]. The two main categories of stroke are ischemic and hemorrhagic. Ischemic stroke is caused by a blockage of blood supply, and hemorrhagic stroke is due to a vascular rupture [2]. A stroke blocks glucose and oxygen supply to the nerve cells, leading to cell death. Ischemic stroke generates reactive oxygen species and causes neuronal damage and apoptosis [3]. Cerebral ischemia prevents the survival signaling pathway and activates the apoptotic signaling pathway, resulting in neuronal cell death [4,5]. Phosphatidylinositol 3 kinase (PI3K) plays a key role in various cellular processes, including metabolism, inflammation, and cell survival [6]. PI3K is responsible for the initiation of a signaling cascade by activating 3-phosphoinositide-dependent kinase 1 (PDK1) and continuously phosphorylating Akt in the activation loop [7]. Akt is a key mediator of signal transduction pathways that regulate cell proliferation and survival. Akt phosphorylates pro-apoptotic proteins, including Bad, glycogen synthase kinase 3 β , and forkhead transcription factor, and prevents apoptotic functions of these proteins [8]. Thus, Akt activation suppresses the activity of caspases and protects cells from apoptosis [9]. Bad is a representative pro-apoptotic protein of the Bcl-2 family and promotes cell death by heterodimerization with Bcl-2 or Bcl-xL [10]. However, the phosphorylated form of Bad (phospho-Bad) has lower capability to interact with Bcl-xL and binds to 14-3-3 proteins [11]. The binding of phospho-Bad and 14-3-3 proteins suppresses cell death by preventing interactions with Bad/Bcl-2 or Bad/Bcl-xL. However, dephosphorylated Bad binds to Bcl-2 or Bcl-xL and continuously releases cytochrome c from mitochondria into the cytosol and initiates the caspase cascade, resulting in apoptosis [12,13].

Chlorogenic acid is a phenolic compound found in various foods such as coffee, cocoa, and citrus fruits [14]. Chlorogenic acid exerts anti-oxidative and anti-inflammatory effects and protects brain tissues from ischemic damage by controlling inflammatory and nerve growth factors [15,16]. We recently reported the antioxidant, anti-inflammatory, and neuroprotective effects of chlorogenic acid on focal cerebral ischemia [17,18]. Furthermore, chlorogenic acid exerts cytoprotective effects against oxidative stress through the PI3K/Akt pathway [19]. The results of the above-mentioned studies provide sufficient evidence regarding the numerous effects of chlorogenic acid. However, the exact neuroprotective mechanism of chlorogenic acid is not fully known. Whether chlorogenic acid regulates the interaction between phospho-Bad and 14-3-3 proteins has not been reported to date. It was hypothesized here that chlorogenic acid exerts neuroprotective effects by regulating the phosphorylation of Akt and Bad and the interaction between phospho-Bad and 14-3-3 proteins. Thus, the changes of phospho-Akt and phospho-Bad expression and of phospho-Bad and 14-3-3 protein binding were investigated in an animal model of focal cerebral ischemia treated with chlorogenic acid.

MATERIALS AND METHODS**Experimental animals and drug treatment**

Male Sprague Dawley rats (200–230 g, n = 60) were purchased from Samtako Co. (Animal Breeding Centre, Osan, Korea). All experimental procedures were carried out according to the guideline of the Institutional Animal Care and Use Committee of Gyeongsang National University (GNU-220222-R0021). Rats were maintained under a controlled environment (25°C, 12 h light/12 h dark cycle) and were provided free access to feed and water. Animals were randomly divided into four groups: vehicle + sham, chlorogenic acid + sham, vehicle +

middle cerebral artery occlusion (MCAO), and chlorogenic acid + MCAO group. Chlorogenic acid (Sigma-Aldrich, USA) was dissolved in phosphate buffer saline (PBS) and was intraperitoneally injected 2 h after the MCAO surgery [16,20]. PBS was used as solvent agent and vehicle-treated animals were injected with PBS without chlorogenic acid. Fifteen rats per group were used for the following experiments: histopathological studies (n = 5 for each group), Western blot (n = 5 for each group), and immunoprecipitation analysis (n = 5 for each group). Neurobehavioral tests were performed in all animals (n = 60).

MCAO

Animals were anesthetized with 50 mg of Zoletil (Virbac, France) before MCAO surgery. They were placed on a heating pad to prevent hypothermia during the surgical procedure. We performed MCAO surgery as previously described manuals [21]. Animals were kept in a supine position and a midline incision was given to the neck. The right common carotid artery (CCA) was exposed by separation from the adjacent muscles, tissues, and nerves. The right external carotid artery (ECA) and the right internal carotid artery (ICA) were continuously exposed and the right CCA was temporarily ligated with microvascular clamp. The proximal end of the right ECA was ligated and cut. A 4/0 nylon suture with rounded tip by heating was carefully inserted into the right ECA and moved forward to the right ICA. It was inserted until resistance was felt to block the origin of the middle cerebral artery. The length of the inserted nylon suture is almost 22–24 mm. The inserted nylon and the ECA were ligated with black silk to fix the nylon suture. The skin of neck was sutured with black silk. Animals were kept on heating pads until they were fully conscious and transferred to animal cage. They were performed neurological behavioral tests 24 h after MCAO and euthanized by cervical dislocation immediately after neurological behavioral tests. The whole brains were carefully isolated from skull and fixed for morphological study. The cerebral cortex tissues were separated from the whole brain and collected further experiments.

Neurological deficit scoring test

A neurological deficit scoring test was carried out for the evaluation of neurological behavior deficits 24 h after MCAO surgery. It was based on a five-point scale system [22]. It was given to animals according to their neurological responses: normal posture and no sign of neurological abnormality (no neurological deficit, 0), lack of the ability to completely extend the contralateral forelimb (mild neurological deficit, 1), circling to the contralateral side (moderate neurological deficit, 2), inability to walk and falling to the contralateral side with signs of seizures and sensitivity to stimulus (severe neurological deficit, 3), and no movement or no sign of consciousness (very severe neurological deficit, 4).

Corner test

The corner test was performed for the examination of sensory-motor asymmetry [23]. Two whiteboards (30 × 20 × 1 cm³) were kept perpendicular at a 30° angle to each other. Small spaces in between the boards were kept for animals to move forward to the corner. Animals were kept at the wide side of the whiteboards and allowed to move freely toward the corner. When the animals reach the corner, their vibrissae was touched to the side of the boards and animals turned to the right or left side. The number of left and right turns for each animal was recorded and the test was repeated ten times. Animals were trained for seven days before MCAO surgery and animals with the same rate of right and left turns were selected for this study.

Adhesive-removal test

Adhesive-removal test was performed using red adhesive dots with approximately 12 mm in diameter for the evaluation of somatosensory sensation [24]. Animals were removed from their cages and kept on a table. They were carefully caught from the neck and red dots were attached to both the forelimbs. They were kept back in their cage and time for the removal of these dots from both the forelimbs was recorded with a stopwatch. The same procedure was repeated five times for each animal. Animals were trained for three days before performing the MCAO surgery and were selected that successfully removed the dots within 10 sec.

Grip strength test

The grip strength test was performed for the evaluation of strength in the left and right forelimbs using a grip strength meter (Jeung Do Bio & Plant Co., Ltd., Korea) [25]. The grip strength meter was set to zero and the right or left forelimb was placed on the metal mesh of the gripper. When the animals grabbed the metal mesh with their right or left paw, we pulled them back from their tails to evaluate maximum force from each forelimb. The test was repeated five times for the left and right paw of each animal.

Hematoxylin and eosin staining

Whole brains were carefully removed from the skull and immediately fixed in a 4% paraformaldehyde solution. They were sliced with a brain matrix (Ted Pella, USA) and washed with tap water for overnight. Tissue slices were dehydrated with graded ethyl alcohol series (70% to 100%) and cleaned in xylene. They were kept in the vacuum chamber of the paraffin embedding center (Leica, Germany) for 1 h and embedded. Paraffin blocks were cut into 4 μ m thick sections using a rotary microtome (Leica). Paraffin ribbons were placed on glass slides and dried on slide warmer (Thermo Fischer Scientific, USA). Section were deparaffinized with xylene, rehydrated in graded ethyl alcohol series (100% to 70%), and kept in tap water. Sections were stained with Harris' hematoxylin solution (Sigma-Aldrich) for 10 min and washed with running tap water for 10 min. They were dipped in a 1% hydrochloric acid solution with 70% ethyl alcohol for differentiation and washed with tap water. They were neutralized by dipping in a 1% ammonia solution and washed with tap water. They were stained with eosin Y solution (Sigma-Aldrich) for 1 min, dehydrated with graded ethyl alcohol series (70% to 100%), and cleaned with xylene. The permount mounting medium (Thermo Fischer Scientific) was dropped and the tissues were covered with cover glass. The sections were observed and photographed using an Olympus microscope (Olympus, Japan). The images of the right cerebral cortex were presented in the results. Five regions of the cerebral cortex were selected and damaged cells were counted in each region. Cells with shrunken dendrite, vacuoles formation, nucleus condensation were consider as damaged cells. Damaged cells were expressed as a percentage of the number of the damaged cells to the number of total cells.

Terminal deoxynucleotidyl transferase dUTP nick end labeling (TUNEL) assay

We performed TUNEL assay to detect apoptotic cell death and TUNEL assay was performed with an ApopTag Peroxidase *In Situ* Apoptosis Detection Kit (Merck, USA) according to the manufacturer's manual. Paraffin sections were deparaffinized with xylene and rehydrated with graded ethyl alcohol series (100% to 70%). Sections were incubated with proteinase K (20 μ g/mL) for 1 min and washed three times with PBS for 5 min. They were dipped in methanol of 3% hydrogen peroxide for 5 min at room temperature, washed three times with PBS for 5 min, and incubated with equilibration buffer for 1 h at 4°C. They were reacted with working strength terminal deoxynucleotidyl transferase (TdT) enzyme in a humidified

chamber for 90 min at 37°C and applied with stop/wash buffer for 10 min to terminate TdT enzyme reaction. They were washed twice with PBS for 5 min and incubated with anti-digoxigenin conjugate in a humidified chamber for 1 h at room temperature. Sections were washed with PBS for three times for 5 min, stained with 3,3'-diaminobenzidine (Sigma-Aldrich), and washed three times with PBS for 5 min. They were counterstained with hematoxylin solution, washed with tap water, dehydrated in graded ethyl alcohol series (70% to 100%), and cleaned with xylene. They were coverslipped with permount mounting medium (Thermo Fisher Scientific, USA) and observed under an Olympus microscope (Olympus). Cells stained with dark brown were considered TUNEL-positive cells. We randomly selected five regions of the cerebral cortex and TUNEL-positive cells were counted in each region. Apoptotic index was expressed as a percentage of the number of the TUNEL-positive cells to the number of total cells.

Western blot analysis

Right cerebral cortex tissues were homogenized in lysis buffer (1% Triton X-100, 1 mM ethylenediaminetetraacetic acid in 1 × PBS [pH 7.4]) containing 200 μM phenylmethylsulfonyl fluoride. Homogenized samples were sonicated for 3 min and centrifuged at 15,000 g for 20 min. The supernatants were collected and the pellets were discarded. Bicinchoninic acid protein assay kit (Pierce, USA) was used to determine the concentration of proteins. Protein assay was performed according to the manufacturer's instructions. Total proteins of 30 μg were kept in ice and loaded into 10% sodium dodecyl sulfate-polyacrylamide (SDS-PAGE) gels for electrophoresis. Samples were electrophorized until the dye went down to the bottom of the gels using mini trans-blot cell electrophoresis (Bio-Rad Laboratories, USA). The gels were removed from glass plate and proteins were transferred into polyvinylidene difluoride (PVDF) membranes in transfer tank for Western blot (Bio-Rad Laboratories). PVDF membranes were reacted with a 5% skim milk solution in tris-buffered saline solution with 0.1% Tween 20 (TBST) for 1 h at room temperature to block non-specific bindings and washed three times with TBST for 10 min. They were incubated overnight at 4°C with following primary antibodies: anti-PDK1, anti-phospho-PDK1, anti-Akt, anti-phospho-Akt, anti-Bad, anti-phospho-Bad, anti-cytochrome c, anti-caspase-3, and anti-β-actin (diluted 1:1,000, Cell Signaling Technology, USA, Santa Cruz Biotechnology, USA). Membranes were washed three times with TBST for 10 min and incubated with horseradish peroxidase-conjugated anti-mouse IgG or anti-rabbit IgG (diluted 1:5,000, Cell Signaling Technology) for 2 h at room temperature. They were washed three times with TBST for 10 min and reacted with chemiluminescence detection reagents (GE Healthcare, UK) for 1 min. Membranes were exposed on X-ray film (Fuji Film, Japan) for 1 min, developed in developer solution (Poohung Photo Chemical, Korea), washed with tap water, and fixed in fixation solution (Poohung Photo Chemical). The detected protein bands were scanned and band intensities were calculated with Image J (Media Cybernetics, USA). The relative integrated density of proteins was expressed as a ratio of the density of proteins to that of β-actin.

Immunofluorescence staining

Paraffin sections were deparaffinized with xylene and rehydrated in graded ethyl alcohol series (100% to 70%). Sections were washed three times with PBS for 10 min and reacted with 1% normal goat serum for 1 h at room temperature for blocking of non-specific antibody bindings. They were washed three times with PBS for 10 min and incubated with anti-phospho-Akt or anti-phospho-Bad (diluted 1:100, Santa Cruz Biotechnology) overnight at 4°C. They were washed three times with PBS and incubated with fluorescein isothiocyanate-conjugated secondary antibody (diluted 1:100, Santa Cruz Biotechnology) for 90 min at room temperature.

Sections were washed three times with PBS for 10 min, reacted with 4',6-diamidino-2-phenylindole (DAPI, Sigma-Aldrich) for 10 min, and cover slipped with fluorescent mounting medium (Agilent Technologies, USA). Stained tissues were observed under a confocal microscope (FV-1000, Olympus) and images were taken from the cortical region. Relative integrated densities were analyzed with Image J (Media Cybernetics) and expressed as a ratio of the integrated density of each animal to that of a vehicle + sham animals.

Immunoprecipitation assay

We performed an immunoprecipitation assay to assess the level of interaction between phospho-Bad and 14-3-3 proteins. Proteins were extracted from the cerebral cortex in the same method that were performed in Western blot analysis. Total protein (200 µg) were reacted with protein A/G agarose beads (Santa Cruz Biotechnology) for blockage of nonspecific binding of other proteins. The mixture was centrifuged at 5,000 g for 1 min and the supernatant was removed. The rest were mixed with anti-14-3-3 antibody and the mixture was incubated for overnight at 4°C on a rocker (FINEPCR CR100, Korea). Protein A/G agarose beads were added in mixture and reacted for 2 h at 4°C. The mixture was washed with radioimmunoprecipitation assay buffer (Sigma-Aldrich) containing PMSF and centrifuged at 10,000 g for 1 min. The supernatant was discarded and sample buffer was added to the rest. Samples were heated at 100°C for 5 min and centrifuged at 10,000 g for 10 min. The supernatant was collected and loaded into a 10% SDS-PAGE gel. They were electrophoresed until the blue dye went down to the bottom of the gel and transferred to PVDF membrane. Membrane was incubated with 5% skim milk solution for 1 h at room temperature and incubated with anti-phospho-Bad antibody (1:1,000, diluted with TBST, Cell Signaling Technology) overnight at 4°C. They were washed three times with TBST for 10 min and reacted with secondary antibody (1:5,000, diluted with TBST, Cell Signaling Technology) for 2 h at room temperature. They were washed three times with TBST for 10 min and reacted with chemiluminescence detection reagents (GE Healthcare). They were exposed on X-ray film (Fuji Film) for 1 min, developed in developer (Poohung Photo Chemical), and continuously fixed in fixer (Poohung Photo Chemical). The detected protein bands were scanned and band intensities were calculated with Image J (Media Cybernetics).

Statistical analysis

All data is represented as mean ± standard error of means. Two-way analysis of variance followed by *post hoc* Scheffe's test was used to analyze the differences among groups. The $p < 0.05$ was considered to be statistically significant.

RESULTS

Neurological tests were performed to assess behavioral deficits and investigate the protective effect of chlorogenic acid on MCAO damage. MCAO animals showed severe neurological deficits such as paralysis, loss of balance, and seizures. However, chlorogenic acid treatment improved these deficits. The neurological deficit scores were 4.09 ± 0.46 and 2.01 ± 0.28 in vehicle + MCAO and chlorogenic acid + MCAO animals, respectively (**Fig. 1A**). Neurological deficits were not found in sham animals regardless of vehicle or chlorogenic acid treatment. The results of the corner test showed a significant increase in the number of right turns in MCAO animals treated with vehicle. However, chlorogenic acid treatment alleviated this increase. The numbers of right turns and left turns were the same in sham animals regardless of vehicle or chlorogenic acid treatment. The number of right turns was 9.16 ± 0.27 and 6.13 ± 0.17

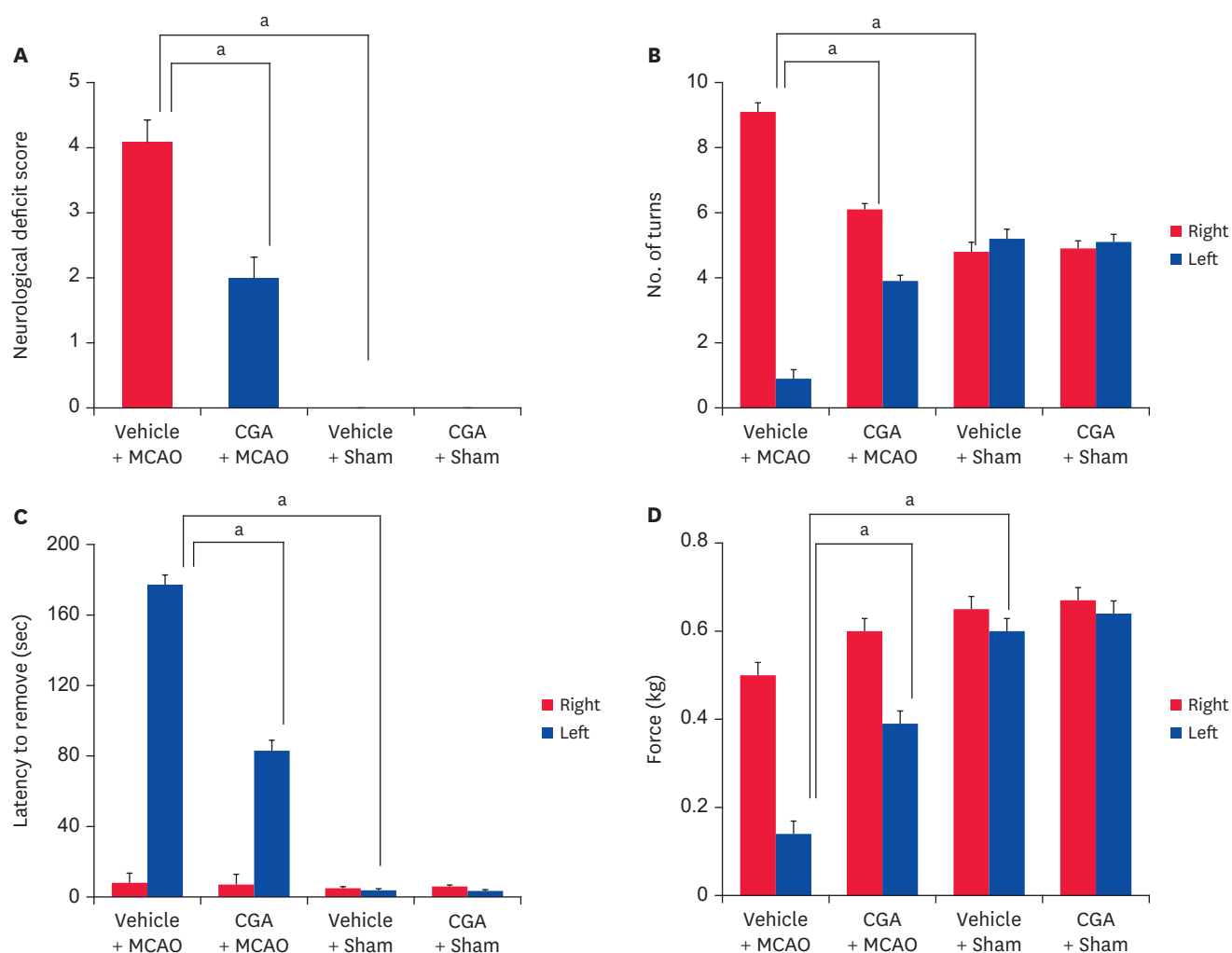


Fig. 1. Neurological deficits scoring test (A), corner test (B), adhesive removal test (C), and grip strength test (D) in vehicle + MCAO, CGA + MCAO, vehicle + sham, and CGA + sham animals. CGA improves neurological behavior deficits in ischemic brain injury. Data ($n = 15$) are shown as the mean \pm standard error of mean. MCAO, middle cerebral artery occlusion; CGA, chlorogenic acid.

^a $p < 0.05$.

in vehicle + MCAO and chlorogenic acid + MCAO animals, respectively (**Fig. 1B**). MCAO damage caused sensory motor impairment. The removal time of red adhesive dots was significantly increased in MCAO animals treated with vehicle; chlorogenic acid treatment alleviated these changes. The time required to remove the adhesive dots was 175.2 ± 8.5 sec and 80.2 ± 6.8 sec in the vehicle + MCAO and chlorogenic acid + MCAO animals, respectively (**Fig. 1C**). In addition, the grip strength test was performed. A decrease in grip strength of the contralateral forelimb was observed in animals with MCAO damage and was alleviated by chlorogenic acid. The grip strength in the left forelimb was 0.14 ± 0.02 and 0.39 ± 0.02 in the vehicle + MCAO and chlorogenic acid + MCAO animals, respectively (**Fig. 1D**). The grip strength of the forelimb was nearly identical in vehicle + sham and chlorogenic acid + sham animals.

In addition, severe structural and histopathological changes were observed in the right cerebral cortex of MCAO animals. Neuronal and cytoplasmic shrinkage, vacuole formation, and shrunken dendrites were observed in MCAO animals (**Fig. 2A-D**). However, chlorogenic acid treatment alleviated the histopathological changes. Sham animals had normal neuronal

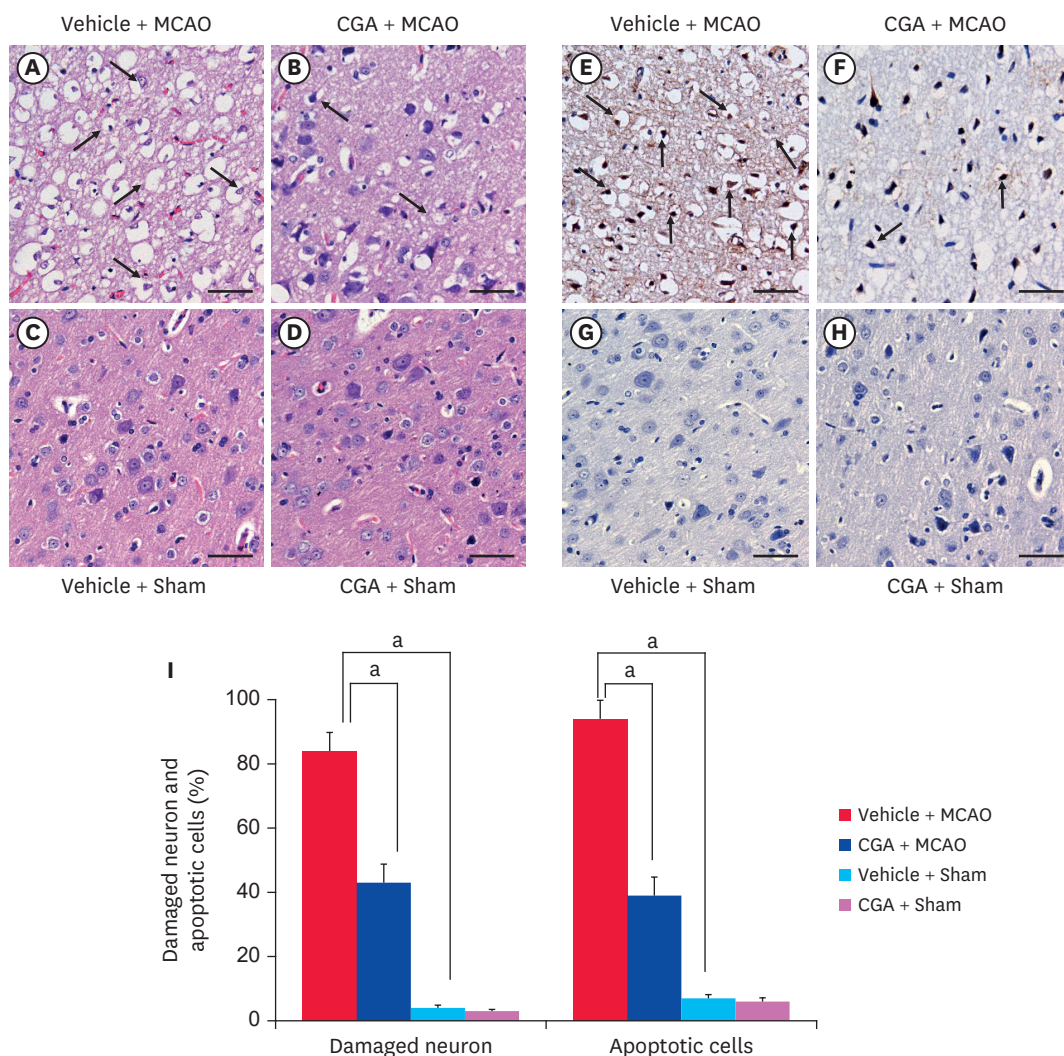


Fig. 2. Representative photograph of hematoxylin and eosin staining (A-D) and TUNEL staining (E-H) of cerebral cortex tissue from vehicle + MCAO, CGA + MCAO, vehicle + sham, and CGA + sham animals. CGA migrated histopathological changes and attenuated increase in the number of TUNEL-positive cells caused by MCAO damage. Arrows indicate shrunken and condensed nuclei. The number of TUNEL-positive cells was markedly increased in vehicle + MCAO animals, while CGA alleviated this increase. Arrows indicate TUNEL-positive cells. Scale bar = 100 μ m. Damaged cells represents the percentage of cells with histopathological lesions to total cells and apoptotic cells represents the percentage of TUNEL-positive cells to total cells (I). Data (n = 4) are shown as the mean \pm standard error of mean. TUNEL, terminal deoxynucleotidyl transferase dUTP nick end labeling; MCAO, middle cerebral artery occlusion; CGA, chlorogenic acid. ^ap < 0.05.

structure with round nuclei and well-developed dendrites. The number of damaged cells was 84 ± 5.77 and 43 ± 5.77 in vehicle + MCAO and chlorogenic acid + MCAO animals, respectively (**Fig. 2I**). TUNEL histochemical staining was performed to detect apoptotic cells. An increase in the number of TUNEL-positive cells was observed in MCAO animals, and chlorogenic acid treatment attenuated the increase (**Fig. 2E-H**). The number of TUNEL-positive cells was 94 ± 6.03 and 39 ± 5.98 in vehicle + MCAO and chlorogenic acid + MCAO animals, respectively (**Fig. 2I**).

The expression of phospho-PDK1, phospho-Akt, and phospho-Bad in the cerebral cortex was analyzed. Western blot analysis showed that MCAO damage decreased phospho-PDK1, phospho-Akt, and phospho-Bad expression, and chlorogenic acid treatment prevented the decrease (**Fig. 3A**). Phospho-PDK1 level was 0.42 ± 0.03 and 1.06 ± 0.05 in vehicle +

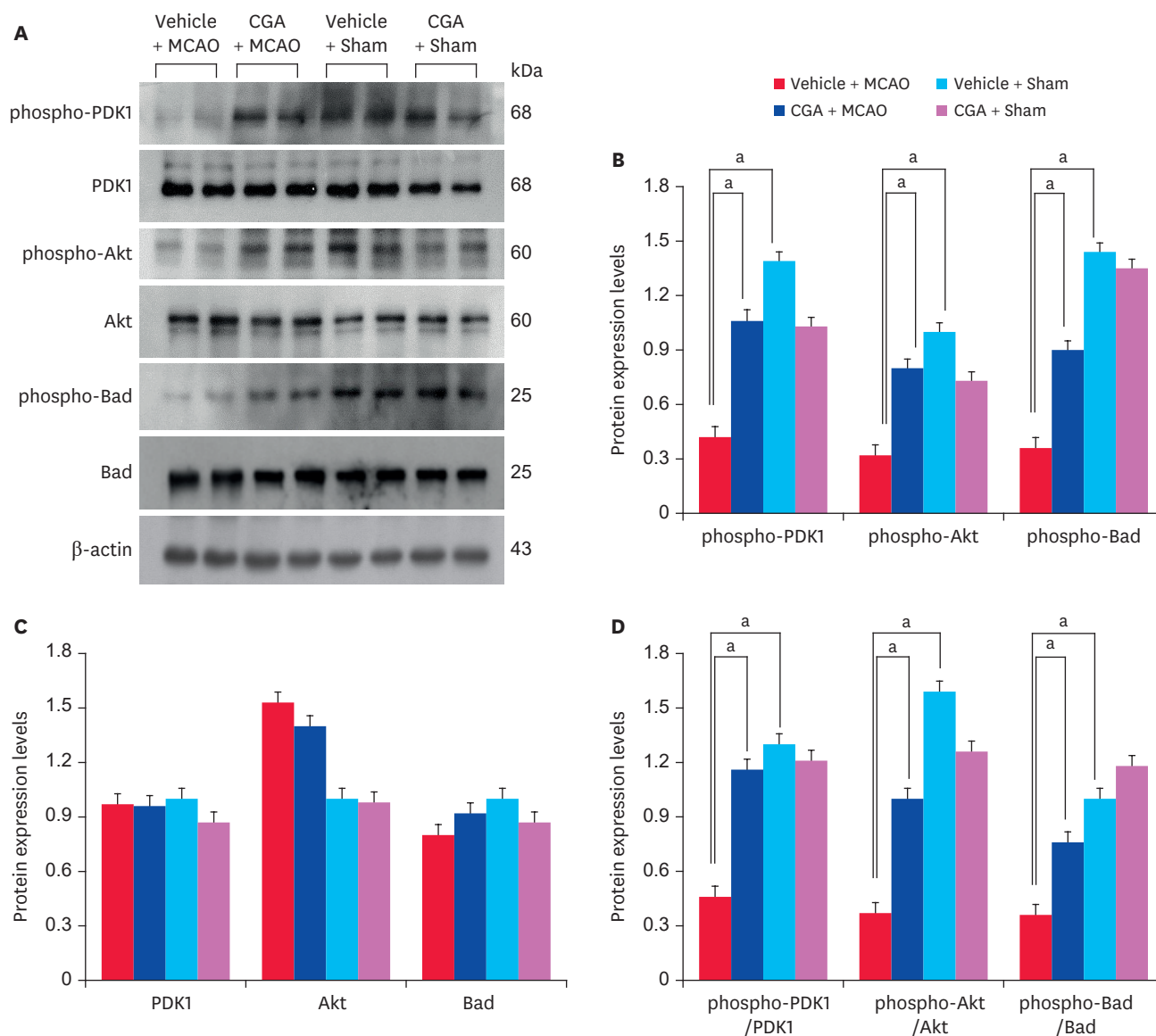


Fig. 3. Western blot analysis of phospho-PDK1, PDK1, phospho-Akt, Akt, phospho-Bad, and Bad in the cerebral cortex from vehicle + MCAO, CGA + MCAO, vehicle + sham, and CGA + sham animals. Each lane represents an individual experimental animal. Densitometric analysis is represented as a ratio of proteins intensity to actin intensity. Molecular weight (kDa) are depicted at right. Data (n = 5) are represented as mean ± standard error of mean. PDK1, phosphoinositide-dependent kinase 1; MCAO, middle cerebral artery occlusion; CGA, chlorogenic acid.

*p < 0.05.

MCAO animals and chlorogenic acid + MCAO animals, respectively (**Fig. 3B**). Phospho-Akt level was 0.32 ± 0.04 in vehicle + MCAO animals and 0.80 ± 0.03 in chlorogenic acid + MCAO animals. Phospho-Bad level was 0.36 ± 0.05 and 0.90 ± 0.03 in vehicle + MCAO and chlorogenic acid + MCAO animals, respectively. The protein expression levels were nearly identical in sham animals regardless of vehicle or chlorogenic acid treatment. Furthermore, PDK1 and Akt expression was maintained at similar levels in vehicle + MCAO animals and chlorogenic acid + MCAO animals. The results of immunofluorescence staining confirmed the change of phospho-Akt and phospho-Bad levels in MCAO animals (**Fig. 4**). DAPI staining was performed to confirm the nucleus, and phospho-Akt and phospho-Bad were located in cytoplasm. These proteins were significantly decreased in the cerebral cortex of MCAO

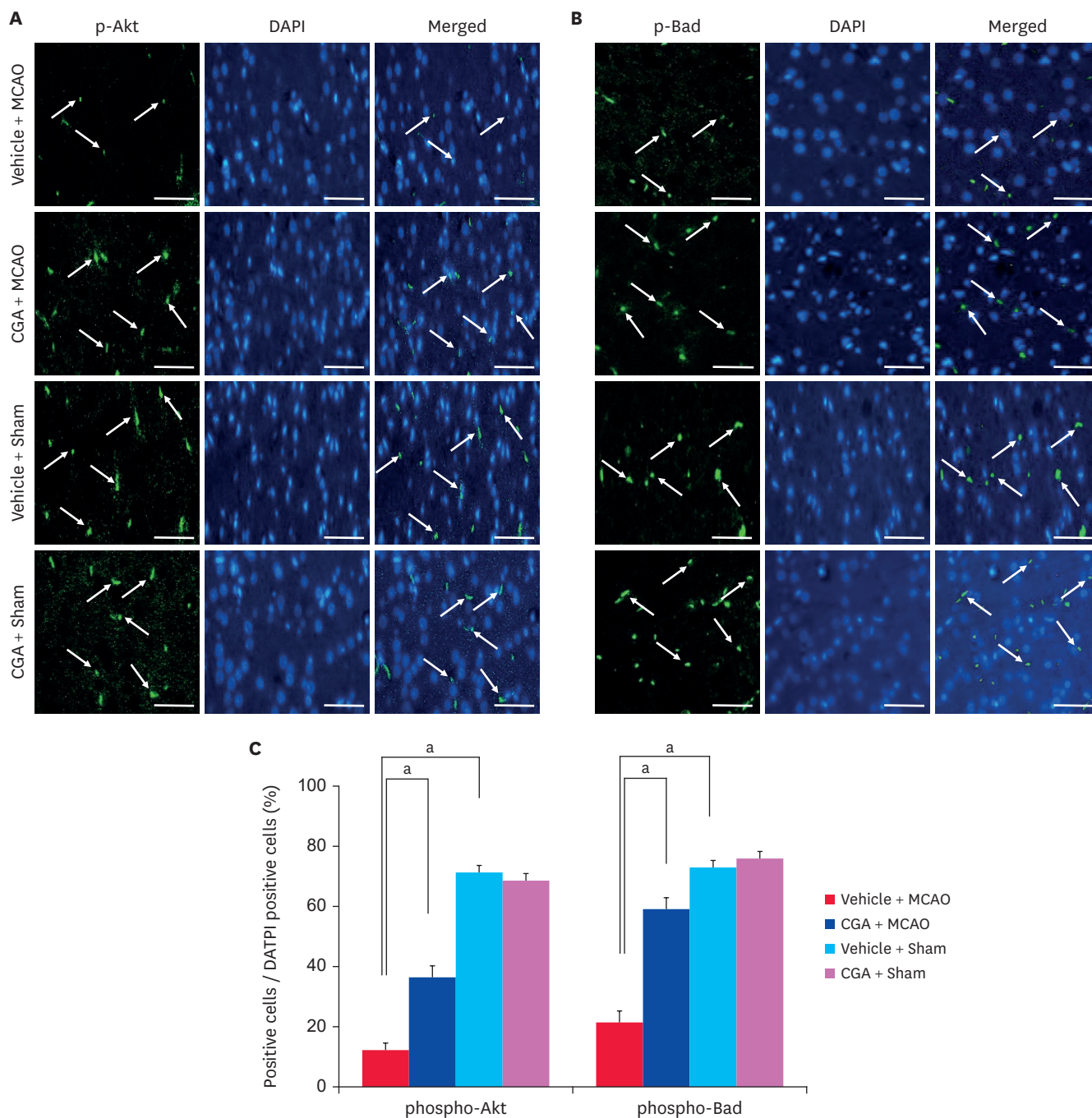


Fig. 4. Immunofluorescence staining of phospho-Akt (A, C) and phospho-Bad (B, C) in the cerebral cortex from vehicle + MCAO, CGA + MCAO, vehicle + sham, and CGA + sham animals. CGA alleviated the decrease of phospho-Akt and phospho-Bad expression due to MCAO damage. The value of positive cells was expressed as a percentage of the number of positive cells to the number of total cells. Arrows indicate positive cells. Data (n = 5) are represented as mean ± standard error of mean. Scale bar = 100 μm.

MCAO, middle cerebral artery occlusion; CGA, chlorogenic acid.

^ap < 0.05.

animals with vehicle treatment, but these decreases were alleviated by chlorogenic acid treatment. The percentage of phospho-Akt-positive cells was 12.17 ± 2.25 and 36.00 ± 4.05 in vehicle + MCAO and chlorogenic acid + MCAO animals, respectively (Fig. 4B). The number of phospho-Bad-positive cells was 21.30 ± 3.55 and 59.24 ± 4.02 in vehicle + MCAO animals and

chlorogenic acid + MCAO animals, respectively (**Fig. 4C**). The number of positive cells was similar between vehicle + sham and chlorogenic acid + sham animals.

Immunoprecipitation analysis was performed to investigate changes in the interaction between phospho-Bad and 14-3-3 proteins in animals with MCAO damage. The interaction level decreased in MCAO animals treated with vehicle but chlorogenic acid treatment alleviated the reduced interaction (**Fig. 5A**). Phospho-Bad and 14-3-3 interaction level was 0.62 ± 0.04 and 1.08 ± 0.05 in vehicle + MCAO animals and chlorogenic acid + MCAO animals, respectively (**Fig. 5B**). Changes in cytochrome c expression were also observed in animals with MCAO damage. Cytochrome c expression was increased in MCAO animals treated with vehicle, and chlorogenic acid treatment alleviated this increase (**Fig. 5C**). Cytochrome c level was 0.91 ± 0.03 in vehicle + MCAO animals and 0.34 ± 0.01 in chlorogenic acid + MCAO animals (**Fig. 5D**). In addition, the expressions of caspase-3 and cleaved caspase-3 were increased, and these increases were alleviated by chlorogenic acid treatment (**Fig. 6A**). Caspase-3 level was 1.32 ± 0.04 and 0.64 ± 0.04 in vehicle + MCAO animals and chlorogenic acid + MCAO animals, respectively (**Fig. 6B**). Cleaved caspase-3 level was 1.06 ± 0.03 in vehicle + MCAO animals and 0.58 ± 0.05 in chlorogenic acid + MCAO animals (**Fig. 6B**). The ratio between cleaved caspase-3 and caspase-3 level was 0.96 ± 0.05 and 0.87 ± 0.07 in vehicle + MCAO animals and chlorogenic acid + MCAO animals, respectively (**Fig. 6C**). Significant difference was not observed between vehicle + sham and chlorogenic acid + sham animals.

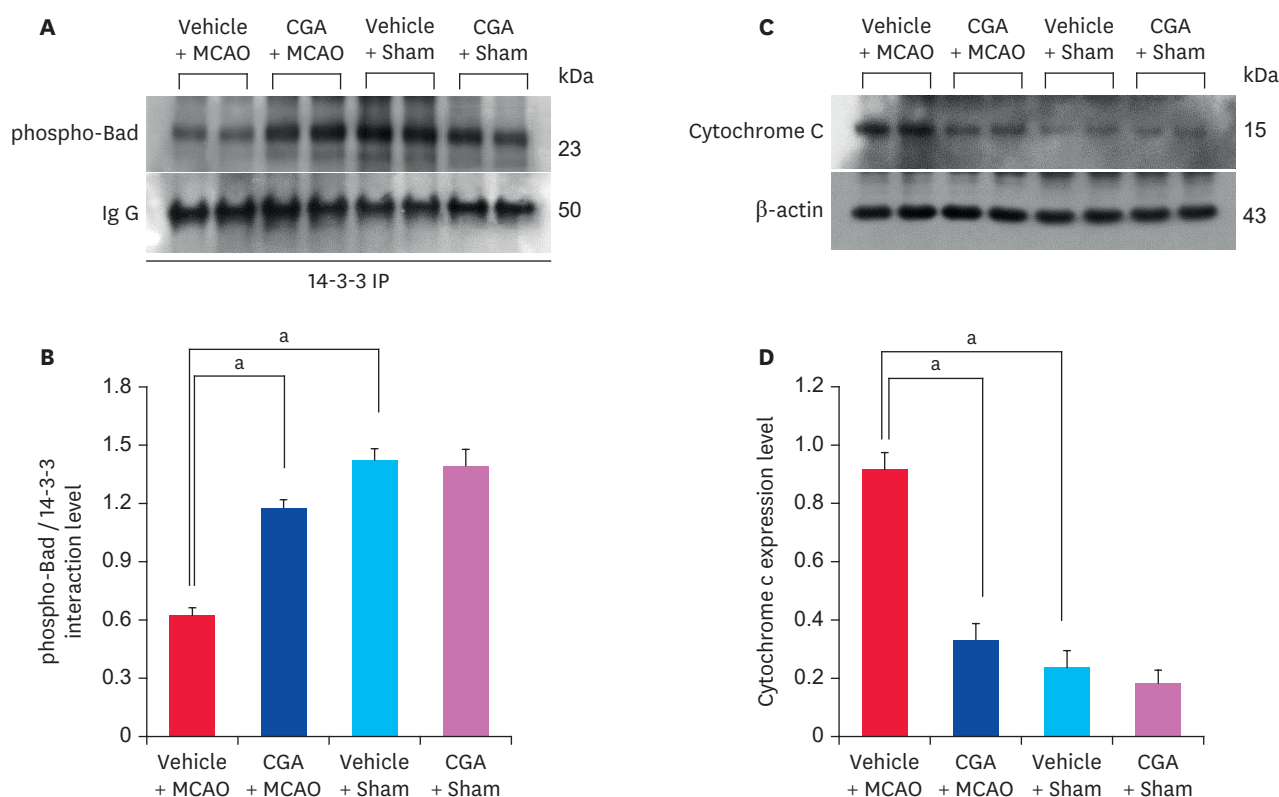


Fig. 5. Immunoprecipitation analysis of phospho-Bad and 14-3-3 binding (A, B) and Western blot analysis of cytochrome c (C, D) in the cerebral cortex from vehicle + MCAO, CGA + MCAO, vehicle + sham, and CGA + sham animals. CGA attenuated the decrease of phospho-Bad and 14-3-3 interaction caused by MCAO damage. Each lane represents an individual experimental animal. Densitometric analysis is represented as a ratio of proteins intensity to IgG or β -actin intensity. Data (n = 5) are represented as mean \pm standard error of mean. MCAO, middle cerebral artery occlusion; CGA, chlorogenic acid. ^ap < 0.05.

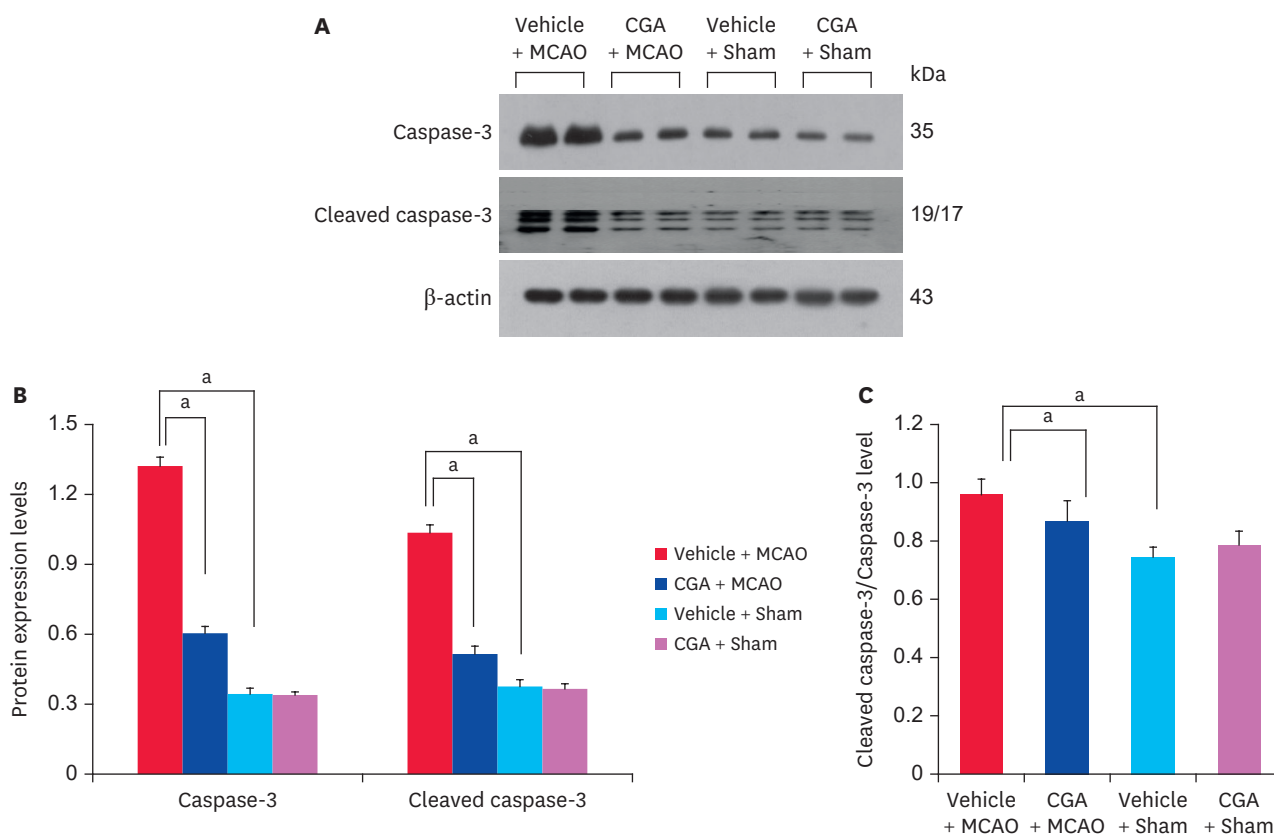


Fig. 6. Western blot analysis of caspase-3 and cleaved caspase-3 in the cerebral cortex from vehicle + MCAO, CGA + MCAO, vehicle + sham, and CGA + sham animals. CGA attenuated the increase of caspase-3 and cleaved caspase-3 caused by MCAO damage. Each lane represents an individual experimental animal. Densitometric analysis is represented as a ratio of β -actin intensity. Data ($n = 5$) are represented as mean \pm standard error of mean. MCAO, middle cerebral artery occlusion; CGA, chlorogenic acid.

^a $p < 0.05$.

DISCUSSION

The neuroprotective effect of chlorogenic acid on cerebral ischemia was confirmed in the present study. Neurological behavior tests were performed to elucidate the neuroprotective function of chlorogenic acid. MCAO damage induced severe neurobehavioral disorders, and chlorogenic acid alleviated these disorders. Chlorogenic acid also prevented histopathological changes and attenuated the number of TUNEL-positive cells in MCAO animals. Chlorogenic acid was confirmed to attenuate the apoptosis process caused by MCAO damage. Activation of the Akt signaling pathway by chlorogenic acid in an animal model of cerebral ischemia was further investigated in the present study.

PI3K plays an important role in cell survival and activates PDK1 [6,7]. The activated PDK1 consecutively activates Akt, which regulates cell proliferation and survival and prevents neuronal cell death. We previously reported that the PI3K/Akt signaling pathway contributes to the neuroprotective effects of various neuroprotective agents in cerebral ischemia [26-28]. Activation of the Akt pathway is an important neuroprotective mechanism in cerebral ischemia. Chlorogenic acid activates the PI3/Akt survival pathway in hydrogen peroxide-induced oxidative stress [19]. Chlorogenic acid represents anti-inflammatory and anti-apoptotic effects against transient cerebral ischemia [29]. Furthermore, chlorogenic acid binds to Akt and regulates downstream proteins including GSK-3 β and FOXO1, and protect

glucose metabolism [30]. In the present study, cerebral ischemia significantly reduced phospho-PDK1 expression and continuously reduced phospho-Akt and phospho-Bad expression. These decreases were mitigated by chlorogenic acid treatment. However, total protein levels did not significantly change in animals with MCAO damage. The results indicate the phosphorylation of these proteins is important for activation of the Akt signaling pathway and of a neuroprotective mechanism during cerebral ischemia. Chlorogenic acid regulates the phosphorylation of these proteins in cerebral ischemia. In addition, the attenuation of decreased phospho-Akt and phospho-Bad levels induced by chlorogenic acid was confirmed using immunofluorescence staining. The number of positive cells was decreased in animals with MCAO damage, and chlorogenic acid prevented the decrease. Activation of phospho-Akt and phospho-Bad is important for cell survival. The results of the present study demonstrate that chlorogenic acid activates the PI3K/Akt signaling pathway and contributes to a neuroprotective mechanism in cerebral ischemia. Bad is a pro-apoptotic protein and a representative downstream target of Akt. Growth or survival factors phosphorylate Bad and attenuate the pro-apoptotic function of Bad. Thus, the attenuation of reduced phospho-Akt and phospho-Bad levels induced by chlorogenic acid in animals with MCAO damage shows the neuroprotective mechanism of chlorogenic acid to be associated with the Akt and Bad signaling pathway.

The phosphorylation of Bad dissociates Bad from the Bcl-xL and Bad complex. The phospho-Bad binds to 14-3-3 proteins and attenuates the pro-apoptotic function of Bad [12]. 14-3-3 interacts with pro-apoptotic proteins such as Bax and Bad [31]. The binding of phospho-Bad and 14-3-3 continuously inhibits cytochrome c release from mitochondria into the cytoplasm, preventing the apoptotic cascade [32]. Thus, the interaction between phospho-Bad and 14-3-3 proteins is important for cell survival and prevents cell death [33]. Results of immunoprecipitation showed a decrease in the interaction between phospho-Bad and 14-3-3 proteins in cerebral ischemia. Chlorogenic acid alleviated the decrease of phospho-Bad and 14-3-3 binding. The results showed that chlorogenic acid regulates binding of phospho-Bad and 14-3-3 proteins in animals with MCAO damage. Maintenance of phospho-Bad and 14-3-3 binding is important for preventing the apoptotic function of Bad and attenuating cell death [32]. However, information regarding the change in phospho-Bad and 14-3-3 binding in the presence of chlorogenic acid during cerebral ischemia is limited. Chlorogenic acid was shown to modulate phospho-Bad and 14-3-3 binding in an animal model of stroke. In addition, chlorogenic acid alleviated MCAO damage-induced increase in cytochrome c and caspase-3. These findings demonstrated the anti-apoptotic effect of chlorogenic acid on cerebral ischemia.

In the present study, chlorogenic acid activated the Akt survival pathway and promoted the interaction between phospho-Bad and 14-3-3 proteins, indicating anti-apoptotic properties. These findings suggest that chlorogenic acid exerts a neuroprotective effect in cerebral ischemia by activating the Akt-Bad signal pathway and maintaining phospho-Bad and 14-3-3 binding.

REFERENCES

1. Ingall T. Stroke--incidence, mortality, morbidity and risk. *J Insur Med.* 2004;36(2):143-152.
[PUBMED](#)
2. Grysiewicz RA, Thomas K, Pandey DK. Epidemiology of ischemic and hemorrhagic stroke: incidence, prevalence, mortality, and risk factors. *Neurol Clin.* 2008;26(4):871-895.
[PUBMED](#) | [CROSSREF](#)

3. Khoshnam SE, Winlow W, Farzaneh M, Farbood Y, Moghaddam HF. Pathogenic mechanisms following ischemic stroke. *Neurol Sci.* 2017;38(7):1167-1186.
[PUBMED](#) | [CROSSREF](#)
4. Broughton BR, Reutens DC, Sobey CG. Apoptotic mechanisms after cerebral ischemia. *Stroke.* 2009;40(5):e331-e339.
[PUBMED](#) | [CROSSREF](#)
5. Chan PH. Mitochondria and neuronal death/survival signaling pathways in cerebral ischemia. *Neurochem Res.* 2004;29(11):1943-1949.
[PUBMED](#) | [CROSSREF](#)
6. Vanhaesebroeck B, Guillermet-Guibert J, Graupera M, Bilanges B. The emerging mechanisms of isoform-specific PI3K signalling. *Nat Rev Mol Cell Biol.* 2010;11(5):329-341.
[PUBMED](#) | [CROSSREF](#)
7. Wick MJ, Dong LQ, Riojas RA, Ramos FJ, Liu F. Mechanism of phosphorylation of protein kinase B/Akt by a constitutively active 3-phosphoinositide-dependent protein kinase-1. *J Biol Chem.* 2000;275(51):40400-40406.
[PUBMED](#) | [CROSSREF](#)
8. Datta SR, Brunet A, Greenberg ME. Cellular survival: a play in three Akts. *Genes Dev.* 1999;13(22):2905-2927.
[PUBMED](#) | [CROSSREF](#)
9. Franke TF, Kaplan DR, Cantley LC. PI3K: downstream AKTion blocks apoptosis. *Cell.* 1997;88(4):435-437.
[PUBMED](#) | [CROSSREF](#)
10. Yang E, Zha J, Jockel J, Boise LH, Thompson CB, Korsmeyer SJ. Bad, a heterodimeric partner for Bcl-XL and Bcl-2, displaces Bax and promotes cell death. *Cell.* 1995;80(2):285-291.
[PUBMED](#) | [CROSSREF](#)
11. Zha J, Harada H, Yang E, Jockel J, Korsmeyer SJ. Serine phosphorylation of death agonist BAD in response to survival factor results in binding to 14-3-3 not BCL-X(L). *Cell.* 1996;87(4):619-628.
[PUBMED](#) | [CROSSREF](#)
12. Datta SR, Katsov A, Hu L, Petros A, Fesik SW, Yaffe MB, et al. 14-3-3 proteins and survival kinases cooperate to inactivate BAD by BH3 domain phosphorylation. *Mol Cell.* 2000;6(1):41-51.
[PUBMED](#) | [CROSSREF](#)
13. Kamada H, Nito C, Endo H, Chan PH. Bad as a converging signaling molecule between survival PI3-K/Akt and death JNK in neurons after transient focal cerebral ischemia in rats. *J Cereb Blood Flow Metab.* 2007;27(3):521-533.
[PUBMED](#) | [CROSSREF](#)
14. Clifford MN. Chlorogenic acids and other cinnamates—nature, occurrence and dietary burden. *J Sci Food Agric.* 1999;79(3):362-372.
[CROSSREF](#)
15. Liang N, Kitts DD. Role of chlorogenic acids in controlling oxidative and inflammatory stress conditions. *Nutrients.* 2015;8(1):16.
[PUBMED](#) | [CROSSREF](#)
16. Miao M, Cao L, Li R, Fang X, Miao Y. Protective effect of chlorogenic acid on the focal cerebral ischemia reperfusion rat models. *Saudi Pharm J.* 2017;25(4):556-563.
[PUBMED](#) | [CROSSREF](#)
17. Shah MA, Kang JB, Park DJ, Kim MO, Koh PO. Chlorogenic acid alleviates cerebral ischemia-induced neuroinflammation via attenuating nuclear factor kappa B activation. *Neurosci Lett.* 2022;773:136495.
[PUBMED](#) | [CROSSREF](#)
18. Shah MA, Kang JB, Park DJ, Kim MO, Koh PO. Chlorogenic acid alleviates neurobehavioral disorders and brain damage in focal ischemia animal models. *Neurosci Lett.* 2021;760:136085.
[PUBMED](#) | [CROSSREF](#)
19. Han D, Chen W, Gu X, Shan R, Zou J, Liu G, et al. Cytoprotective effect of chlorogenic acid against hydrogen peroxide-induced oxidative stress in MC3T3-E1 cells through PI3K/Akt-mediated Nrf2/HO-1 signaling pathway. *Oncotarget.* 2017;8(9):14680-14692.
[PUBMED](#) | [CROSSREF](#)
20. Lee K, Lee JS, Jang HJ, Kim SM, Chang MS, Park SH, et al. Chlorogenic acid ameliorates brain damage and edema by inhibiting matrix metalloproteinase-2 and 9 in a rat model of focal cerebral ischemia. *Eur J Pharmacol.* 2012;689(1-3):89-95.
[PUBMED](#) | [CROSSREF](#)
21. Longa EZ, Weinstein PR, Carlson S, Cummins R. Reversible middle cerebral artery occlusion without craniectomy in rats. *Stroke.* 1989;20(1):84-91.
[PUBMED](#) | [CROSSREF](#)

22. Shamsaei N, Erfani S, Fereidoni M, Shahbazi A. Neuroprotective effects of exercise on brain edema and neurological movement disorders following the cerebral ischemia and reperfusion in rats. *Basic Clin Neurosci.* 2017;8(1):77-84.
[PUBMED](#) | [CROSSREF](#)
23. Michalski D, Küppers-Tiedt L, Weise C, Laignel F, Härtig W, Raviolo M, et al. Long-term functional and neurological outcome after simultaneous treatment with tissue-plasminogen activator and hyperbaric oxygen in early phase of embolic stroke in rats. *Brain Res.* 2009;1303:161-168.
[PUBMED](#) | [CROSSREF](#)
24. Zhang L, Chen J, Li Y, Zhang ZG, Chopp M. Quantitative measurement of motor and somatosensory impairments after mild (30 min) and severe (2 h) transient middle cerebral artery occlusion in rats. *J Neurol Sci.* 2000;174(2):141-146.
[PUBMED](#) | [CROSSREF](#)
25. Takeshita H, Yamamoto K, Nozato S, Inagaki T, Tsuchimochi H, Shirai M, et al. Modified forelimb grip strength test detects aging-associated physiological decline in skeletal muscle function in male mice. *Sci Rep.* 2017;7(1):42323.
[PUBMED](#) | [CROSSREF](#)
26. Park DJ, Kang JB, Shah FA, Koh PO. Resveratrol modulates the Akt/GSK-3 β signaling pathway in a middle cerebral artery occlusion animal model. *Lab Anim Res.* 2019;35(1):18.
[PUBMED](#) | [CROSSREF](#)
27. Koh PO. Melatonin prevents hepatic injury-induced decrease in Akt downstream targets phosphorylations. *J Pineal Res.* 2011;51(2):214-219.
[PUBMED](#) | [CROSSREF](#)
28. Koh PO. Ferulic acid prevents the cerebral ischemic injury-induced decrease of Akt and Bad phosphorylation. *Neurosci Lett.* 2012;507(2):156-160.
[PUBMED](#) | [CROSSREF](#)
29. Lee TK, Kang JJ, Kim B, Sim HJ, Kim DW, Ahn JH, et al. Experimental pretreatment with chlorogenic acid prevents transient ischemia-induced cognitive decline and neuronal damage in the hippocampus through anti-oxidative and anti-inflammatory effects. *Molecules.* 2020;25(16):3578.
[PUBMED](#) | [CROSSREF](#)
30. Gao J, He X, Ma Y, Zhao X, Hou X, Hao E, et al. Chlorogenic acid targeting of the AKT PH domain activates AKT/GSK3 β /FOXO1 signaling and improves glucose metabolism. *Nutrients.* 2018;10(10):1366.
[CROSSREF](#)
31. Samuel T, Weber HO, Rauch P, Verdoodt B, Eppel JT, McShea A, et al. The G2/M regulator 14-3-3sigma prevents apoptosis through sequestration of Bax. *J Biol Chem.* 2001;276(48):45201-45206.
[PUBMED](#) | [CROSSREF](#)
32. Downward J. How BAD phosphorylation is good for survival. *Nat Cell Biol.* 1999;1(2):E33-E35.
[PUBMED](#) | [CROSSREF](#)
33. Fan J, Xu G, Nagel DJ, Hua Z, Zhang N, Yin G. A model of ischemia and reperfusion increases JNK activity, inhibits the association of BAD and 14-3-3, and induces apoptosis of rabbit spinal neurocytes. *Neurosci Lett.* 2010;473(3):196-201.
[PUBMED](#) | [CROSSREF](#)